CHAPTER 294

MODELLING OF 3D SEDIMENT TRANSPORT IN THE SURF ZONE

by

Berry Elfrink [1], Ida Brøker[1], Rolf Deigaard [2], Erik Asp Hansen[1] and Peter Justesen[1]

ABSTRACT

The three-dimensional sediment transport in the surf zone has been investigated using two different approaches for modelling of the flow pattern. The first approach is based on the integrated momentum concept for the turbulent wave-current boundary layer, see Fredsøe (1984), the second approach is based on the k-model, as described in Deigaard et al. (1991). The k-model allows for a more consistent description of the time and space varying eddy viscosity than the integrated momentum approach, but demands considerably more computation effort. The driving forces are calculated according to the formulations of Deigaard et al. (1991) and Deigaard (1993). The model based on the integrated momentum equation is able to reproduce the details of the flow satisfactorily. The presence of a longshore current increases the turbulence near the bed. This results in a decreased offshore directed flow velocity near the bed and an increase in the sediment concentration. Comparisons with field measurements show good agreement.

INTRODUCTION

When waves break turbulent kinetic energy is produced at the water surface. This energy is partly dissipated in the surface roller and partly transported downwards into the water column. The radiation stress gradients, associated with the wave breaking, are balanced by the pressure gradient originating from the wave setup and the mean bed shear stress.

In case of uniform conditions along the shore, the net discharge in the mean cross shore flow must balance the fluid mass transported in the surface roller and the discharge associated with the asymmetric wave motion and streaming in thc bottom boundary layer. The zero mass flux in the cross shore direction is achieved by a slope of the mean water level. The vertical variation of the cross shore flow velocity is therefore charaterized by offshore directed velocities near the bed (the undertow) and onshore velocities further away from the bed.

---

[1] Danish Hydraulic Institute, Agern Allé 5, DK-2970 Hørsholm, Denmark

[2] Institute of Hydrodynamics and Hydraulic Engineering, Technical University of Denmark, 2800 Lyngby, Denmark

In the longshore direction, the forces associated with the wave breaking can only be balanced by a mean bed shear stress which drives the wave induced longshore current.

The interaction of the turbulence originating from wave breaking with the turbulence generated in the bottom boundary layer is of great importance in the description of the sediment transport in the surf zone, see Justesen et al. (1986). Due to the higher level of turbulence more sediment can be kept into suspension under breaking waves than under non-breaking waves.

In the present work, the flow conditions along the shore are assumed to be uniform, see figure 1. The waves approach the coast under an angle α and are assumed to be long crested and monochromatic.

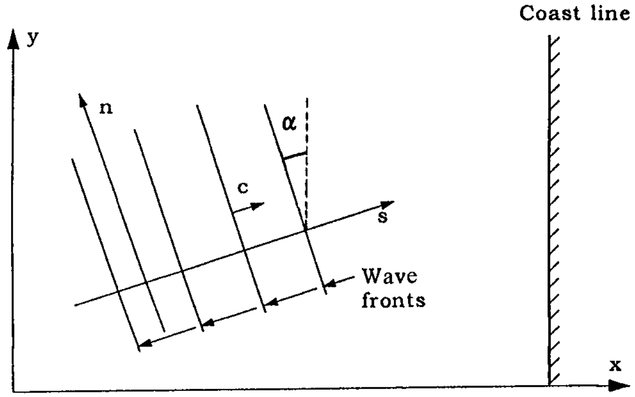

Figure 1 : plan view

VERTICAL VARIATION OF THE DRIVING FORCE

Deigaard and Fredsøe (1989) determined the time mean shear stress in normally incident breaking waves. It was found that the vertical transfer of horizontal momentum gives a significant contribution to the momentum balance. Deigaard (1993) derived expressions for the time mean shear stress in case of oblique waves by considering the momentum balance for the surface rollers. The surface shear stress is given as :

$$\frac{\overline{\tau_s}}{\rho} = \left(-\frac{g}{8c}\frac{d\,H^2 c}{ds} - \frac{d}{ds}\frac{Ac}{T} \right) \begin{pmatrix} \cos\alpha \\ \sin\alpha \end{pmatrix} \tag{1}$$

where H=wave height, s=direction of wave propagation, A=surface roller cross section, c=wave celerity, α=wave angle, g=gravitational accelleration and T=wave period.

The cross shore and longshore components of the time mean bed shear stress are determined by the gradients in the radiation stress and the mean water surface slope, the wave set-up, in the cross shore direction, Justesen et al. (1994) :

$$\frac{\bar{\tau}_{b,x}}{\rho} = -\frac{g}{8}\frac{dH^2}{dx}\cos^2\alpha - \frac{g}{16}\frac{dH^2}{dx} - \frac{d}{dx}\left(\frac{Ac}{T}\right)\cos^2\alpha - gDs_s \tag{2}$$

$$\frac{\bar{\tau}_{b,y}}{\rho} = -\frac{g}{8}\frac{dH^2}{dx}\cos\alpha\sin\alpha - \frac{d}{dx}\left(\frac{Ac}{T}\right)\cos\alpha\sin\alpha \tag{3}$$

Here, s_s is the slope of the water surface, and x and y are the cross shore and longshore coordinate, respectively. The shear stress varies linearly across the water column. The vertical distribution of the time mean shear stess is illustrated in figure 2.

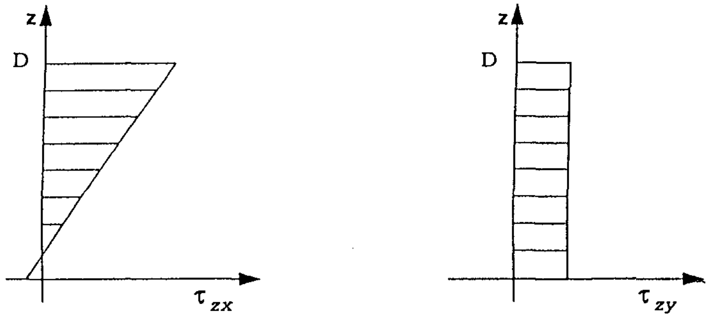

Figure 2 : Illustration of the time mean shear stress in the cross shore and longshore direction.

In both models, the wave orbital motion was calculated from linear wave theory, but any potential wave theory could be used here. If a non-linear wave description is used, the mean bed shear stress associated with the wave motion is non-zero. In the model based on the integrated momentum equation, the wave motion outside the boundary layer is described by potential theory. In order to fulfil the requirements of potential theory, the mean bed shear stress due to the wave motion must be zero. Brøker-Hedegaard et al. (1991) showed that a perfect force balance can be obtained by adding a small constant velocity to the orbital motion. This additional velocity is found iteratively by the requirement of zero mean bed shear stress, see Elfrink et al. (1993). In the K-model, this velocity is found automatically.

In case of progressive waves, a small net shear stress is generated due to the non-uniformity of the wave boundary layer. Brøker-Hedegaard (1985) showed that this streaming induced shear stress at the bed can be expressed as :

$$\tau_{str.} = \frac{\rho}{c} \overline{U_o U_f |U_f|} \tag{4}$$

where U_o= wave orbital velocity and U_f= instantaneous friction velocity.

THE INTEGRATED MOMENTUM APPROACH

In this model the instantaneous velocity profiles and eddy viscosity profiles inside the boundary layer are assumed to be given by a logarithmic and a parabolic distribution, respectively. The interaction of the undertow, the longshore current and the waves is taken into account by superposing the wave by a steady current and solving the turbulent boundary layer for the combined wave/current motion. The total mean eddy viscosity has contributions from the wave breaking, from the bottom layer and from the mean current. The eddy viscosity due to the mean current outside the boundary layer is calculated by applying the mixing length concept. The equations are solved by the assumption that the net flux perpendicular to the shoreline is zero. It is noted that the integrated momentum approach is by far the most computationally efficient.

The time-averaged flow velocity distribution is calculated from the vertical distribution of the driving forces (eq. 1 - 4) and the mean eddy viscosity :

$$\frac{d\vec{U}}{dz} = \frac{\vec{\tau}}{\rho \nu_t} \tag{5}$$

The three contributions to the eddy viscosity are calculated independently from each other. The contribution from the wave boundary layer is calculated from the boundary layer model of Fredsøe (1984). The contribution from the mean flow is modelled by applying a mixing length concept, see Justesen et al. (1994) and the eddy viscosity due to wave breaking is calculated from the transport equation for turbulent kinetic energy, see Deigaard et al. (1986).

THE K-EQUATION MODEL

The k-model approach in the present work is an extension of the model developed by Deigaard et al. (1991) for the case of normally incident waves.

The driving force in the unsteady motion is composed of a steady part as given in eqs. 1 - 4 and an oscillatory part which is given by the periodically varying horizontal pressure gradient associated with the wave motion. The flow equations, neglecting convective terms, read :

$$\frac{\partial u}{\partial t} = -\frac{1}{\rho}\frac{\partial p}{\partial x} + \frac{1}{\rho}\left[\frac{\partial \tau_{zx}}{\partial z} - \frac{\partial \overline{\tau}_{zx}}{\partial z}\right] \tag{6}$$

$$\frac{\partial v}{\partial t} = -\frac{1}{\rho}\frac{\partial p}{\partial y} + \frac{1}{\rho}\left[\frac{\partial \tau_{zy}}{\partial z} - \frac{\partial \overline{\tau}_{zy}}{\partial z}\right] \tag{7}$$

where u=cross shore flow velocity, v=longshore flow velocity, u=cross shore coordinate, y=longshore coordinate, z=vertical coordinate, p=pressure gradient associated with the wave motion, ρ=density of water, τ_{zx} and τ_{zy} = cross shore and longshore components of the shear stress respectively, t = time.

$$\tau_{zx} = \rho \nu_t \frac{\partial u}{\partial z} \quad ; \quad \frac{1}{\rho}\frac{\partial p}{\partial x} = -\frac{\partial U_o}{\partial t} \tag{8}$$

$$\tau_{zy} = \rho \nu_t \frac{\partial v}{\partial z} \quad ; \quad \frac{1}{\rho}\frac{\partial p}{\partial y} = -\frac{\partial V_o}{\partial t} \tag{9}$$

The eddy viscosity, ν_t, is calculated from the diffusion equation for turbulent kinetic energy, see Justesen et al. (1994) :

$$\nu_t = l\sqrt{k} \quad ; \quad \frac{\partial k}{\partial t} = -\frac{\partial}{\partial z}\left(\frac{\nu_t}{\sigma_n}\frac{\partial k}{\partial z}\right) + \frac{1}{\rho} PROD - c_l \frac{k^{\frac{2}{3}}}{l} \tag{10}$$

PROD = production term, which consists of contributions from wave breaking , as expressed through the gradient in wave energy flux, E_f, and from the shear stress in the model.

$$PROD = \tau_{zx}\frac{\partial u}{\partial z} + \tau_{zy}\frac{\partial v}{\partial z} - \frac{\partial E_f}{\partial x} \tag{11}$$

SEDIMENT TRANSPORT

The sediment transport is calculated according to Fredsøe et al. (1985) and Deigaard et al. (1986). Here the bed load transport model of Engelund and Fredsøe (1976) is used, where the bedload transport is calculated from the instantaneous bed shear stress. The vertical variation of the suspended sediment concentration is calculated from the vertical diffusion equation for suspended sediment.

The omission of the convective terms in the diffusion equation is alleviated by adding the lagrangian flow velocity times the mean concentration to the time averaged product of instantaneous velocity and concentrations.

COMPARISON OF THE 2 MODELS

Figs 3 and 4 show the mean cross shore and longshore flow velocities for the 2 models for varying wave angles. The wave height in this example was taken as 0.6 m and the period as 6 s. The water depth was 1 m and the bed roughness 0.5 mm. The energy dissipation, the surface roller volume and the cross shore gradient of the surface roller were calculated by using a wave height gradient of -0.015 and a bed slope of 0.033. The sediment grain size was taken as 0.2 mm.

It can be seen that the agreement between the two models is good. In the lower part of the water column, the gradients in the velocity profiles are somewhat steeper for the k-model than for the integrated momentum approach, which indicates slightly higher values of the eddy viscosity for the latter.

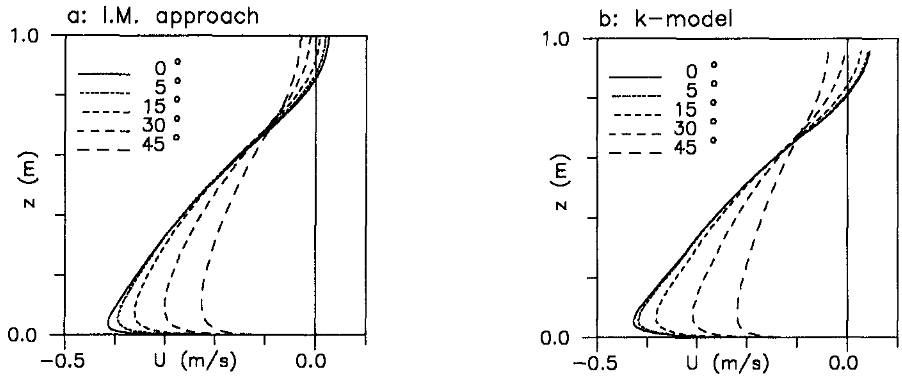

Figure 3 : Time averaged cross shore flow velocities for the two models.
a = integrated momentum approach , b = k-model.

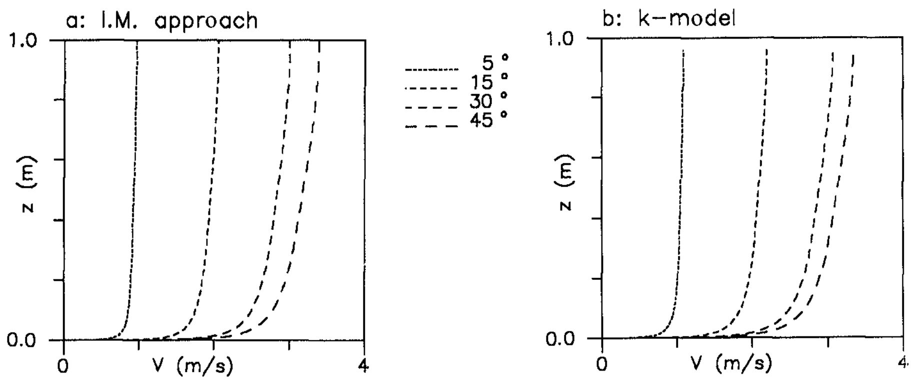

Figure 4 : Time averaged longshore flow velocities for the two models.
a = integrated momentum approach, b = k-model.

The time variation of the cross shore and longshore components of the friction veloctiy are shown in figs. 5 and 6. For low angles of wave incidence, the cross shore friction velocities are slightly lower under the wave crest for the integrated momentum approach than for the k-model, but generally the agreement is good.

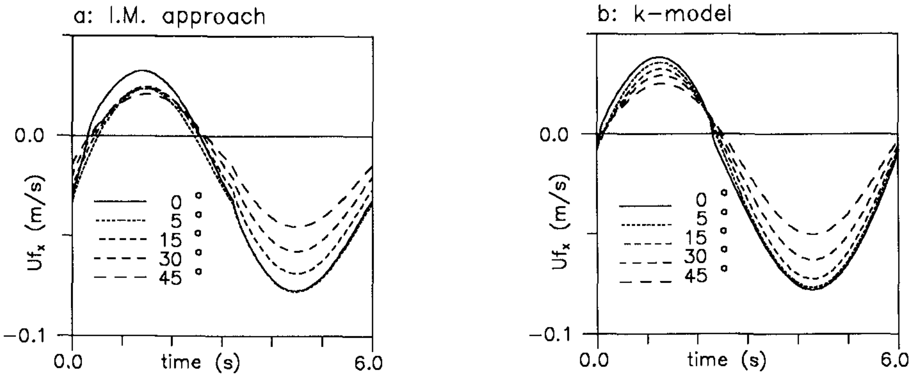

Figure 5 : Time variation of the cross shore component of the shear velocity. a = integrated momentum approach, b = k-model.

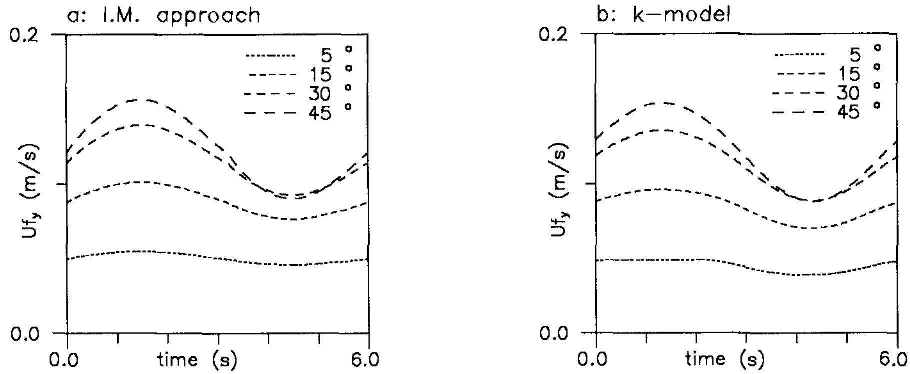

Figure 6 : Time variation of the longshore component of the shear velocity. a = Integrated momentum approach, b = k-model.

In this example, the cross momentum exchange of horizontal momentum, associated with the gradients in the longshore current velocity across the shore has been neglected. This causes unrealistically high values of the calculated longshore current velocites and friction velocities. Usually, the mean bed shear stress is calculated from a surf zone model which includes this momentum exchange. However, this has no importance in the context of intercomparing the two different models.

In both models, the suspended sediment transport is calculated as the product of the instantaneous flow velocities and the instantaneous sediment concentration :

$$q_s = \frac{1}{T}\int_0^T\int_0^D (uc)\, dzdt \tag{12}$$

In the calculation of the sediment transport in the surf zone, the vertical variation of the suspended sediment concentration is important. Deviations in the time averaged suspended sediment concentrations may occur due the phase difference between the flow in the wave boundary layer and the outer flow. In the k-model, this phase difference is included, whereas the boundary layer in the integrated momentum approach is assumed to be in phase with the outer flow. Figs. 7 and 8 show the time averaged vertical variation of the suspended sediment fluxes for the two models in the cross shore and longshore direction. The agreement is seen to be good for all examined wave angles.

A number of comparisons was performed were the hydrodynamic parameters (e.g the wave height, period, angle of incidence and energy dissipation) were varied systematically. Also different grain sizes were analyzed. The integrated momentum approach tends to give slightly higher transport rates for high levels of turbulence, associated with wave breaking. This is due to the different techniques in determining the turbulence originating from the boundary layer, the mean flow and wave breaking. Generally the agreement is good.

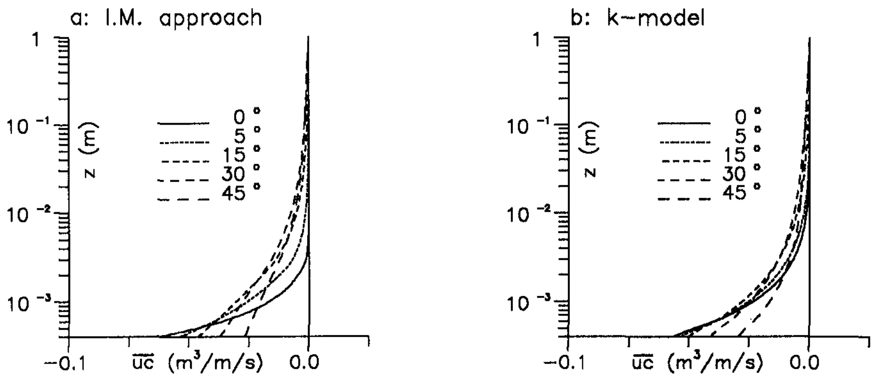

Figure 7 : Vertical variation of the time averaged cross shore sediment flux. a = Integrated momentum approach, b = k-model.

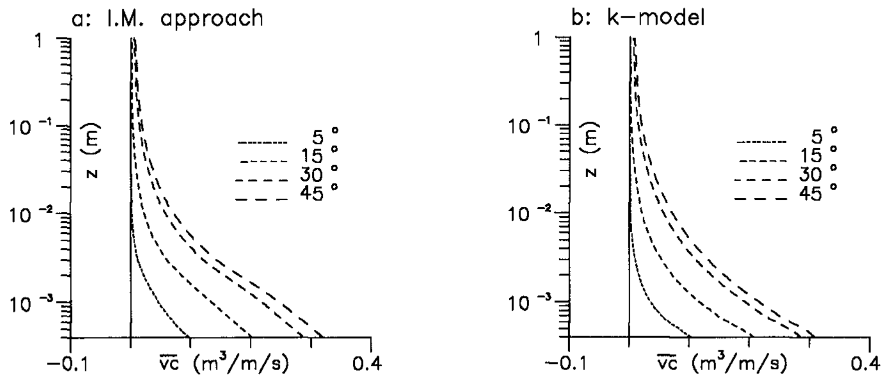

Figure 8 : Vertical variation of the time averaged longshore sediment flux.
a = Integrated momentum approach, b = k-model.

It can be concluded that the integrated momentum approach gives results very similar to the more complete k-model in determining the mean flow, the time variation of the bed shear stess and the sediment transport.

THE INTERACTION OF UNDERTOW AND LONGSHORE CURRENT

The presence of a longshore current will affect the undertow and the resulting cross shore sediment transport. The interaction of the longshore current with the undertow is important in the determination of the cross shore profile evolution. The longshore current causes higher levels of turbulence near the sea bed, this affects the vertical shape of the cross shore velocity as the vertical velocity gradients decrease due to the higher eddy viscosity. This results in a reduction of the near bed cross shore flow velocity. At the same time, the higher levels of turbulence allow higher concentrations of suspended sediment.

A test was performed with the model based on the integrated momentum equation for a situation with and without the presence of a longshore current of 0.5 m/s. In the present example, a wave height of 0.7 m and a period of 5 s was used. The water depth is 1.5 m and the energy dissipation corresponds to the energy loss in a hydraulic jump. Figure 9a shows the simulated time averaged cross shore velocity profile with and without a longshore current. In both cases, the mean flow under the wave crest balances the mass transport in the surface roller and the wave drift. It can be seen that the near bed offshore directed velocities are lower in case of a longshore current. Consequently, the velocities in the vicinity of the water surface are slightly higher.

The bed concentrations for both cases are shown in figure 9b. The main difference is that the bed concentration does not vanish at the flow reversal (t/T ≈ 0.05, and t/T ≈ 0.45) in case of a longshore current. The bed concentrations are lower under the wave crest (t/T < 0.5) than under the trough (t/T >0.5) because the wave orbital motion and the undertow counteract each other, whereas they both are directed offshore under the wave trough. The maximal bed concentration is slightly higher in case of a longshore current. The vertical variations of the time-mean sediment concentration for the two examples are shown in figure 9c. The increased eddy viscosity and the higher mean bed concentration result in a higher mean concentration in case of a longshore current. The combined effect of lower offshore velocities near the bed and the higher sediment concentrations result in an increased cross shore sediment transport in case of a longshore current in this example as shown in figure 9d.

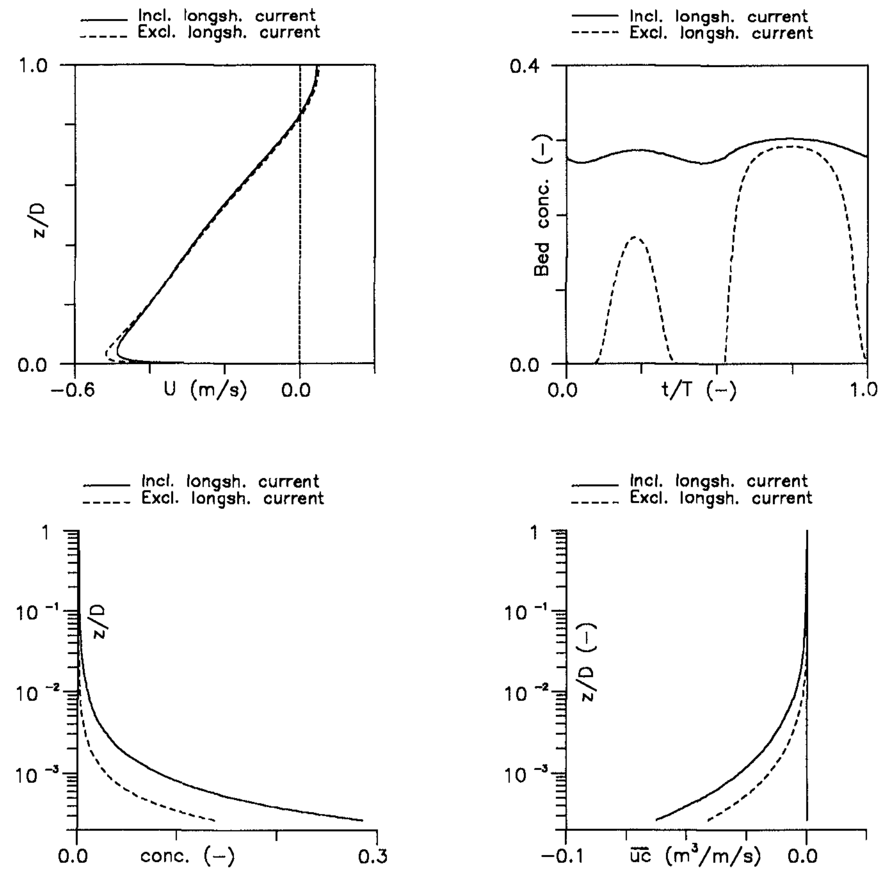

Figure 9 : Interaction of the undertow with a longshore current. a: Mean cross shore flow, b: time variation of the bed concentration, c: time-mean sediment concentration d: time-mean sediment flux.

COMPARISON WITH FIELD MEASUREMENTS

A comparison was made with measured flow velocity profiles at the Ebro delta, Spain, which were reported in Rodriguez et al. (1994). The comparison was made for three levels of calibration. First, the mean cross shore flow velocities were calculated without any calibration. In these simulations, a fully developed roller, where the associated energy dissipation corresponds to the energy loss in a stationary hydraulic jump was assumed.

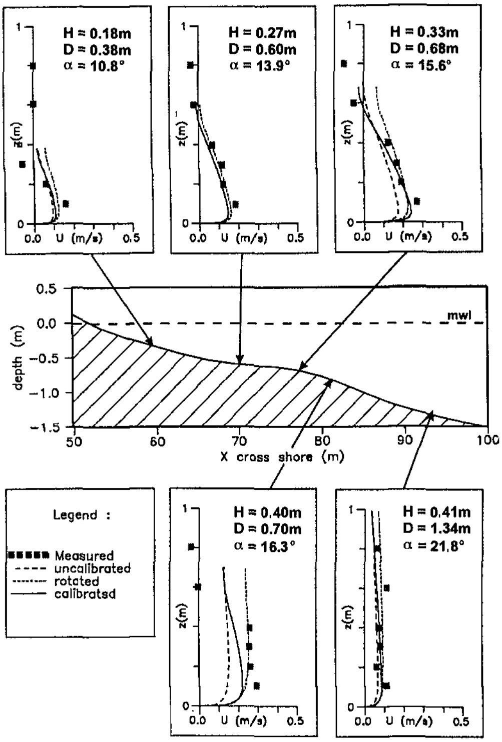

Figure 10 : Comparison of the present model with field measurements from Rodriguez et al. (1994). Three levels of calibration were applied : 1 - uncalibrated, 2 - rotated, 3 - adjusted roller volume.

secondly, the uncalibrated flow velocity profiles were rotated such that the calculated depth averaged velocity matched the measured values. This adjustment accounts for possible 2D effects, e.g. the coast is not perfectly uniform in the longshore direction. Thirdly, a calibration was performed by determining the volume of the surface rollers from the measured mean cross shore flow velocity and the estimated wave drift, which was calculated from sinusoidal wave theory. In all cases the waves were assumed to be unidirectional and regular. The wave orbital motion was calculated by using 1st order Stokes theory. The results for the mean cross shore flow are shown in figure 10. Generally the agreement is satisfactorily. The uncalibrated model underestimates the measured velocities near the bed slightly. The rotation of the coordinate system improves the agreement to a limited degree. The agreement is worst for the sample point located at a cross shore coordinate of approximately 80 m. For the present test, this corresponds to the outer surf zone. The calibrated velocity profiles match the velocity gradients better than the uncalibrated model.

CONCLUSIONS

A numerical model was developed for the flow and the sediment transport under oblique incident waves in the surf zone. The model is based on the integrated momentum equation for the wave boundary layer of Fredsøe (1984). The eddy viscosity consists of contributions from the wave boundary layer, the mean flow and wave breaking. These contributions are calculated separately.

The model based on the integrated momentum equation gives very similar results compared to a more complete turbulence model. For engineering purposes, the integrated momentum approach is recommended because it is able to reproduce the details of the flow and the sediment transport and is very efficient in computing time.

In case of a longshore current the level of turbulence near the bed is increased compared to a situation without current. This results in lower near bed velocities of the undertow and an increased concentration of suspended sediment.

Comparison of the simulated mean cross shore and longshore flow velocities show good agreement with field measurements.

ACKNOWLEDGEMENT

This work was supported by the Danish Technical Research Council (STVF) under the program “Marin Teknik”.

The authors would like to express their gratitude to Andres Rodriquez for supplying the data of the field measurements at the Ebro delta.

REFERENCES

Brøker Hedegaard, I. (1985). Wave generated Ripples and resulting Sediment Transport in Waves. Series paper no 36. Institute of Hydrodynamics and Hydraulic Engineering (ISVA). Technical University of Denmark.

Brøker Hedegaard, I. , R. Deigaard, and J. Fredsøe (1991). Onshore/Offshore sediment transport and morphological modelling of coastal profiles. Proc. Coastal Sediments '91, ASCE, Seattle, pp. 643-657

Deigaard, R. , J. Fredsøe and I. Brøker Hedegaard (1986). Suspended sediment in the surf zone. J. Waterway, Port, Coastal and Ocean Engineering, ASCE, vol. 112 (1), pp 115-128

Deigaard, R and J. Fredsøe (1989). Shear stress distribution in dissipative water waves. Coastal Engineering, ASCE, vol. 13, pp 357-378

Deigaard, R. (1993). A note on the 3-dimensional shear stress distribution in a surf zone. Coastal Engineering, vol. 20, pp 157-171.

Deigaard, R., P. Justesen, J. Fredsøe (1991). Modelling of the undertow by a one equation turbulence model. Coastal Engineering, vol. 15, pp 431-458.

Elfrink, B., I.Brøker Hedegaard, R. Deigaard and J. Fredsøe. (1993). Net sediment transport in non-breaking waves. Progress report no 74. Institute of Hydrodynamics and Hydraulic Engineering (ISVA). Technical University of Denmark. pp 1-10.

Engelund, F and J. Fredsøe (1976). A sediment transport model for straight alluvial channels. Nordic Hydrology, vol 7, pp 293 - 306

Fredsøe, J. (1984). Turbulent boundary layers in wave-current motion. Journal of Hydraulic Engineering, ASCE, vol. 110 (HY8), pp 1103-1120.

Fredsøe, J., O.H. Andersen and S. Silberg. (1985) . Distribution of suspended sediment in large waves. J. of Waterways, Port, Coastal and Ocean Engineering, ASCE, vol. 111 (6), pp 1041 - 1059.

Justesen, P., J. Fredsøe and R. Deigaard. (1986). The bottleneck problem for turbulence in relation to suspended sediment in the surf zone. Proc. 20th Coastal Engineering Conference, Taipei, Vol 2, pp 1225 - 1239.

Justesen, P., E.A. Hansen, I. Brøker and R. Deigaard. (1994). Longshore and cross shore velocity profiles in spilling breakers with an oblique angle of incidence. Progress report no 75. Institute of Hydrodynamics and Hydraulic Engineering (ISVA). Technical University of Denmark. pp 41-54.

Rodriguez A., A. Sánchez-Arcilla, F.R. Collado, V. Gracia, M.G. Coussirat, J. Prieto. Waves and currents at the Ebro delta surf zone: Measurements and modelling. Proc. 24th Int. Conf. on Coastal Eng. 1994. pp. 268-269